Rotary Kiln Transport Processes

John R. Ferron
Dept. of Chemical Engineering, University of Rochester, Rochester, NY 14627

Dilip K. Singh
Dept. of Chemical Engineering, Youngstown State University, Youngstown, OH 44555

Slow rotation of a cylindrical kiln, partially filled with powder or granular solid, produces a planar interface between the bulk of the solid and the gas phase, tilted at the angle of repose. Particles cascade downward on this plane, moving relatively freely and randomly, providing the principal mechanism for particulate diffusion and mixing in the kiln. The plane is also the most favorable location for chemical reactions that require efficient gas-solid heat and mass transfer. Conservation equations are constructed for planar and bulk regions, coupled by the particulate exchange produced by rotation. Sample problems of mixing and heat exchange illustrate problem formulation and useful simplifications. A penetration model predicts wall-to-bed heat transfer coefficients, leading to better agreement with experiment than is obtained when planar processes are omitted.

Introduction

Rotary kilns are employed in a variety of processes involving combinations of particulate mixing and gas-solid or solid-phase reaction with intensive heat and mass transfer. Calcination, pyrolysis, and sintering, generally endothermic reactions controlled by combinations of heat addition and rate of absorption or elimination of gas, are typical and classical examples. Kilns are operated with continuous feed and discharge, pitched slightly from inlet to outlet, normally running less than half-full of solid. The upper space accommodates a countercurrent flow of hot gas which may serve both to supply the heat of reaction and to provide reactant or carry off gaseous products.

The top plane of the solid phase is evidently the most likely region for the highest rates of transfer, providing an excellent receptor for both convective and radiative heat transfer and facilitating mass transfer to the contiguous gas phase.

The top plane is also the active region for particulate mixing in the system, the one location at which individual particles or small clumps are relatively free of surrounding solids and may move randomly, so as to permit dispersion of particles of different composition.

A previous study (Singh, 1978) used a two-dimensional model based on methods of the kinetic theory of gases to characterize particle interactions on the top plane and to define a particulate diffusion coefficient appropriate when particle population is quite small—conditions produced ordinarily by a low rate of vessel rotation. The diffusion coefficient thus defined serves as the basis for the prediction of diffusivities for denser conditions on the top plane, permitting general correlation of the applicable experimental data within their precision.

Previous studies of rotary kilns have often produced models used to simulate or rationalize chemical and transport processes. Mu and Perlmutter (1980, 1981), for example, developed a one-dimensional form describing the bulk flow and dependent on just the axial variable. Rotational processes and flow over the top plane tend to equalize conditions laterally, so that the one-dimensional description is useful.

In the present work we include more detail about particle movement on the top plane and in the bulk, permitting multidimensional representations. The objective is a set of conservation equations that includes diffusional terms and permits a wider variety of problems to be framed and solved. We illustrate uses with problems of particulate mixing and of heat transfer.

Top-Plane and Bulk-Phase Flows

Particle exchange rate

Prior studies have noted that movement of solid is quite regular both in axial flow and with rotation of the kiln. Packing

Correspondence concerning this article should be addressed to J. R. Ferron.

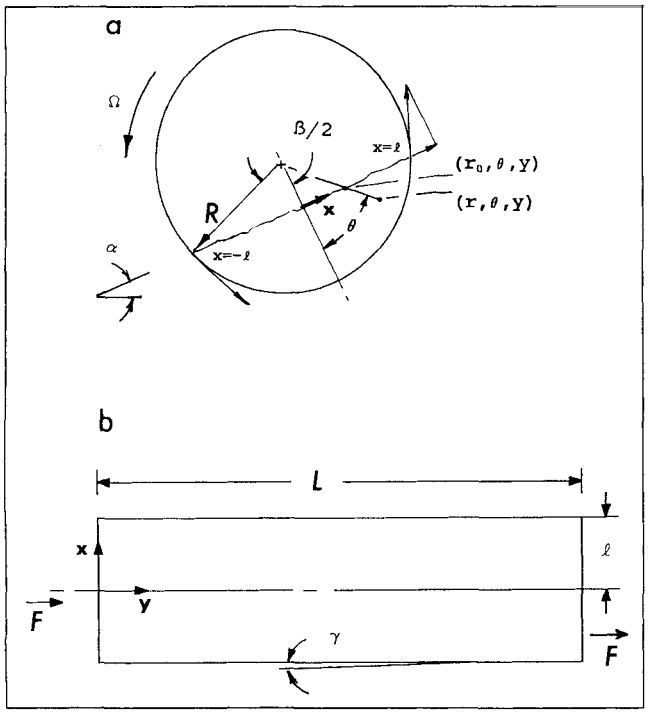

Figure 1. Rotary kiln.

a. Cross section
b. Lateral view
(x, y) top-plane coordinates
(x, y, r) or (r, θ, y) coordinates of bulk of solid α angle of repose
Degree of fill is determined by angle β
γ axial pitch of kiln
Tangential vector at $x=\ell$ suggests how additional top-plane momentum is supplied by rotation, then is removed at $x=-\ell$

in the bulk of the solid is sufficiently dense to cause the particulate mass to respond to rotation as an almost completely rigid body. There is friction between the particles and the vessel wall sufficient to cause the solid phase to be tilted laterally by rotation, at the angle of repose. Internal devices may be installed to assist this process and to discourage the periodic slumping of the bed that might otherwise occur. Axial movement of the solid is not strongly deterred by wall friction, however, and internals may be designed to induce flow at the wall and to promote plug flow in the axial direction. The resulting flat velocity profile is perturbed only moderately by percolation and other rearrangement phenomena.

Thus, the bulk of the particulate solid is transported by relatively rigid rotational and axial motions. These two mechanisms provide little opportunity for mixing, most of which must take place on the top plane. This has been illustrated in an experiment involving mixing of tracer particles: blocking axial movement on the top plane, but not in the bulk, reduced the diffusion coefficient of the mixing process by more than 90% (Singh, 1978). Photographic experiments have been especially helpful in portraying the action of the top plane in producing lateral mixing (Bridgwater, 1976; Lehmberg et al., 1983; Oyama, 1980), which is facilitated by the rapid downward flow of particles, so that lateral fluxes are several times larger than axial values.

Figure 1 suggests a cross section of the solid phase and a plan view of the top plane. From the cross-section geometry we may calculate that the volumetric flow onto the top plane resulting from one complete revolution is given by

$$2\pi L \int_{(R^2-\ell^2)^{1/2}}^{R} r\,dr = \pi\ell^2 L$$

where ℓ is the half-width of the top plane and L and R are respectively kiln length and radius. For spherical particles of diameter σ, having void fraction in the bulk ϵ, the corresponding particle flow onto the top plane, that is, for $x>0$ in Figure 1, equal to that returning to the bulk in $x<0$, is $N_p=6(1-\epsilon)\ell^2 L\Omega/\sigma^3$, where Ω is the rotational rate. Later we make use of this particulate exchange flux in several ways as we consider the interactions of bulk solid and the top plane.

The importance of the top plane in mixing and reaction may be examined by calculating how frequently the bulk of solid is turned over by flows across the top plane. The fraction of the vessel volume filled by solid, f, is given by $f=(\beta-\sin\beta)/\pi$, where the angle β is defined in Figure 1. The volumetric flow to the top plane divided by the volume of solid in the vessel is the rotational turnover ratio, $V^*=(\ell/R)^2/f$. Fraction filled and ℓ/R are related through β by $\ell/R=\sin(\beta/2)$.

Figure 2 is a plot of V^* in terms of f showing, for example, that the particulate contents of the vessel are passed across the top plane three to five times per revolution at common operating conditions of $f=0.15$ to 0.3. Exposure to the gas is evidently much more frequent than one might initially suppose. Moreover, there are multiple opportunities with each revolution for axial displacement of particles by collisions on the top plane. Despite plug flow in the bulk, axial mixing in the kiln can be very good.

The exchange flux, N_p, is the total for half the top plane. Thus, if we define the local particulate flux, $N(x, y)$, where x is the lateral coordinate of Figure 1 and y is the axial coordinate measured from the inlet end of the kiln, then

$$N_p=\frac{6(1-\epsilon)\ell^2 L\Omega}{\sigma^3}=\int_0^L\int_0^\ell N(x, y)\,dx\,dy \qquad (1)$$

where the upper limit of the inner integral may be either $+\ell$ or $-\ell$. Because ϵ, L, Ω, and σ are constants, we may solve the integral equation by inspection, obtaining

$$N(x)=\frac{12(1-\epsilon)\Omega x}{\sigma^3} \qquad (2)$$

Here we abbreviate $N(x, y)$ to $N(x)$, noting that no y-dependence has been included; properties of the cross section of Figure 1 are assumed to be independent of the axial coordinate. The expression for the local particulate flux is valid for $-\ell\le x\le\ell$. The function is antisymmetric in x, $N(-x)=-N(x)$.

Average residence times

The time required for rotation of a particle depends on its position on the negative half of the top plane, and we may obtain the value by reference to Figure 1. Thus,

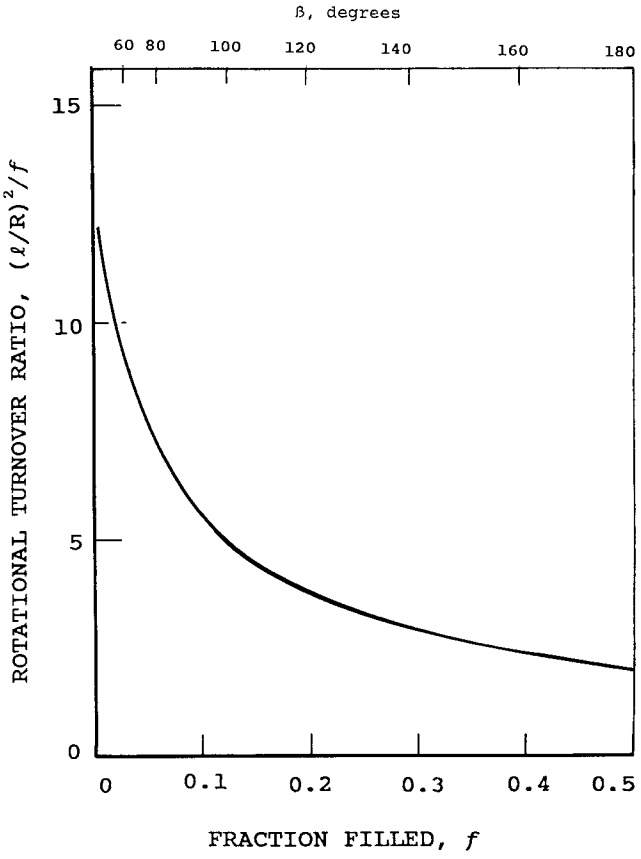

Figure 2. Rotational turnover ratio as a function of fraction filled.

Ratio is number of times per revolution that vessel contents appear on top plane

$$\tau(x)=\frac{1}{\pi\Omega}\tan^{-1}\frac{x}{(R^2-\ell^2)^{1/2}} \tag{3}$$

is the time for rotation of a particle from a negative top-plane value of x to the corresponding positive position, from coordinates $(-x, y)$ to (x, y). We note that $\tau(x)\le\beta/2\pi\Omega$. And because the vessel is likely to be operated less than half full, so that $\beta\le\pi$, we note that $\tau(x)\le 1/2\Omega$—frequently, but not necessarily, a small number compared to common batch times for transient kiln operation or average residence times for continuous use.

A particle makes several excursions over the top plane and through the bulk during each revolution of the vessel. The average total time for each such excursion is $1/V^*\Omega=fR^2/\ell^2\Omega$.

The total is the sum of the average residence times for movement across the top plane and for rigid rotation through the bulk phase. The first of these was estimated for sparsely populated top planes by Singh (1978) as $(4/3)\ell/V_m$, where $v_m=1.6186(g\ell\sin\alpha)^{1/2}$ is the mean speed of a particle on the top plane, with g the acceleration of gravity and α, Figure 1, the angle of repose. Thus we have the two average residence times, τ_{top} and τ_{rot} for the top plane and for rotation, respectively, as

$$\tau_{top}=\frac{4\ell}{3v_m} \tag{4a}$$

$$\tau_{rot}=\frac{fR^2}{\ell^2\Omega}-\frac{4\ell}{3v_m} \tag{4b}$$

Some values are listed in Table 1. Notice that the time spent by a particle on the top plane may be much smaller than required for rotation.

Conservation Equations

Mass balances for surface and bulk regions

We may now define the local density of particles on the top plane at time, t, as $n(x,y,t)$ and construct the continuity equation representing the density function. This is

$$\frac{\partial n}{\partial t}+\nabla\cdot nv=N \tag{5}$$

where v, with components v_x and v_y, is the local mass-average velocity of the particle flow on the top plane and the divergence is taken with respect to coordinates x and y, where $-\ell\le x\le\ell$, $0\le y\le L$, $t\ge 0$.

The average density on the top plane for low rotational rates has been estimated (Singh, 1978) to be

Table 1. Average Particle Residence Times*

f	R m	Ω s^{-1}	$\ell\Omega/v_m$	$(\ell/R)^2/f$	τ_{top} ms	τ_{rot} s
0.15	1	1/30	0.01	4.4	14	6.8
		1/10	0.03	4.4	41	2.2
0.15	0.05	1/30	0.002	4.4	3	6.8
		1/10	0.007	4.4	9	2.3
		1/3	0.023	4.4	30	0.65
0.3	1	1/30	0.01	3.0	15	10.0
		1/10	0.03	3.0	44	3.3
0.3	0.05	1/30	0.002	3.0	3	10.0
		1/10	0.007	3.0	10	3.3
		1/3	0.025	3.0	33	1.0

*g = 9.8 ms^{-2}, α = 20 degrees

$$n_{av}=\frac{2.471\ell^{3/2}(1-\epsilon)\Omega}{\sigma^3(g\sin\alpha)^{1/2}} \tag{6}$$

We use this estimate here for all conditions considered.

Coordinates appropriate to the bulk phase are also illustrated in Figure 1. We may use (x,r,y), where r is radial distance from the center of the vessel's cross section, to represent a point in the bulk. Alternatively we may use polar coordinates, (r,θ,y). In either case we employ subscript 0 to indicate surface conditions when we relate these to bulk coordinates. Thus, certain identities are helpful later when we employ the conservation equations. In the bulk

$$\theta=\sin^{-1}\frac{x}{r} \tag{7a}$$

and relating surface and bulk we write

$$\frac{x_0}{r_0}=\frac{x}{r} \tag{7b}$$

$$r_0=(R^2+\ell^2+x_0^2)^{1/2} \tag{7c}$$

Ordinarily there is no need for the subscript on x_0, and we use it only to avoid ambiguity.

The bulk phase has the continuity equation,

$$\frac{\partial n_b}{\partial t}+\nabla\cdot n_b v_b=0 \tag{8}$$

where v_b has components v_{br}, $v_{b\theta}$, and v_{by} (or v_{bx}, v_{by}, and v_{br}) and the divergence is also defined for either three-dimensional coordinate system. Equation 8 is valid for $r_0\le r\le R$, $-\beta/2\le\theta\le\beta/2$, $0\le y\le L$, $t\ge 0$.

A common circumstance is that of constant bulk density, $n_b=$ constant, for which case Eq. 8 has the form

$$\nabla\cdot v_b=0 \tag{9}$$

a kind of incompressible flow.

Local properties of particulate mixtures

Mixing in rotary kilns involves the blending of particles having narrow, unimodal distributions of sizes. Bimodal or multimodal distributions are only slowly altered, and the direction of change may be toward segregation rather than blending. This occurs for unusually large particles in the bottom half of the inclined top plane, where reincorporated particles must be trapped by gaps in the bulk-phase packing in order to be rotated around to positive x. Large particles have relatively low probabilities of reincorporation, and they tend to segregate in a pool at $x=-\ell$. Fines also segregate, collecting in the voids of the bulk phase, so that they do not regularly flow over the top plane.

Differences among particles of about the same size are frequently chemical, therefore representing different participants or stages in reaction. Whereas in the former case just a few reactants are typically involved, one might in the latter case expect to consider many stages. In calcination there is a continuum of species, each one having a different extent of reaction—a different core size, for example, of unreacted solid. In the following we presume that in practice a relatively small, discrete set of species is sufficient as a model of the common processes, although there is no limit in theory.

Thus, we set $n_i(x,y,t)$ m^{-2}, $i=1, 2, \ldots, I$, equal to the local surface density of particles of species i. The comparable quantity in the bulk is n_{bi} m^{-3}, as usual related to either variable set, (x,r,y,t) or (r,θ,y,t).

Species and enthalpy balances

Diffusion occurs on the top plane with effective diffusivity D_i. That is, the top-plane flux of species i is

$$J_i=-nD_i\nabla\frac{n_i}{n}+n_i v \tag{10a}$$

If $I=1$, only one particle species is present, and we set $D_i=0$.

We assume that diffusion is not significant in the bulk. This flux is entirely convective,

$$J_{bi}=n_{bi}v_b \tag{10b}$$

The diffusivity, D_i m^{2}s^{-1}, may be estimated from the empirical correlation

$$D_i=0.81D_s\,n_{av}^{0.43} \tag{11a}$$

where the limiting value for sparsely populated surface conditions, achieved when $\ell^{3/2}\Omega/[\sigma(g\sin\alpha)^{1/2}]\le 0.5$, usually meaning small values of the rotation rate, is (Singh, 1978)

$$D_s=\frac{0.00540(g\sin\alpha)^{1/2}\ell^{3/2}\sigma^2}{fR^2(1-\epsilon)} \tag{11b}$$

A differential area, $dxdy$, at (x,y) on the positive half of the top plane receives particles from the bulk region at the rate $N\,dxdy$. A similar area at $(-x,y-v_{by}\tau)$ was the source of the same particles. Here $\tau=\tau(x)$, given by Eq. 3, is the time needed for rigid rotation from $-\theta_0$ to θ_0. The motion is actually helical, hence the increment in the y coordinate.

Similarly the flux of species i onto the top plane may be represented by $[n_{bi}(x,r_0,y,t)/n_b]N$, which we abbreviate to $n_{bi0}N/n_b$ for later use. As a consequence of the rigid-body rotation and helical advance,

$$\frac{n_{bi0}}{n_b}\equiv\frac{n_{bi}(x,r_0,y,t)}{n_b(x,r_0,y,t)}=\frac{n_i(-x,y-v_{by}\tau,t-\tau)}{n(-x,y-v_{by}\tau,t-\tau)} \tag{12}$$

The value of r_0 is given by Eq. 7c, where x_0 is the same as x of Eq. 12.

Utilizing these definitions, we may construct the particulate species balances on the top plane,

$$\frac{\partial n_i}{\partial t}+\nabla\cdot n_i v=nD_i\nabla^2\frac{n_i}{n}+H(x)\frac{Nn_{bi0}}{n_{b0}}+H(-x)\frac{Nn_i}{n}+R_i \tag{13}$$

where $H(x)=0$, $x<0$, $H(x)=1$, $x>0$, is the Heaviside step

function and R_i is the rate of production of species i per unit area by chemical reaction.

The corresponding particulate species balance for the bulk phase is

$$\frac{\partial n_{bi}}{\partial t} + \nabla \cdot n_{bi} v_b = R_{bi} \tag{14}$$

where R_{bi} is the rate of appearance of i per unit volume of the bulk. As stated previously, no diffusion is considered. One might include on the righthand side a term involving $D_{bi}\nabla^2 n_{bi}$ to represent the relatively small contributions of diffusion to particulate flux in the bulk. A value of D_{bi} might be estimated to be about $0.1D_i$ on the basis of the blocked-surface experiment mentioned earlier.

When n_b is constant, as in Eq. 9, and no reaction occurs, Eq. 14 expresses the constancy of n_{bi} following the motion of rigid-body rotation on the range $-\beta/2 \le \theta \le \beta/2$.

The enthalpy of the particles may be represented by $h_i(x,y,t)$ for the top plane and by $h_{bi}(x,y,r,t)$ for the bulk. Both may be calculated as the sum of sensible heat relative to a datum temperature and heat of formation at the datum. We define enthalpies of the particle flows as $h = \Sigma_i h_i n_i/n$ and $h_b = \Sigma_i h_{bi} n_{bi}/n_b$. Temperatures are T and T_b for top plane and bulk, respectively.

The energy balance for the top plane, neglecting mechanical terms, is

$$\frac{\partial (nh)}{\partial t} + \nabla \cdot (nhv) = n \sum_{i=1}^{I} D_i \nabla \cdot h_i \nabla \frac{n_i}{n} + N[H(x)h_{b0} + H(-x)h] + Q \tag{15}$$

where Q is the combined convective and radiative heat flux onto the top plane. We treat D_i as a constant and set $h_{b0} \equiv h_b(x,r_0,y,t)$ for $x>0$. This is the enthalpy of the particle flow into the top plane at the point of emergence.

For the bulk phase

$$\frac{\partial (n_b h_b)}{\partial t} + \nabla \cdot (n_b h_b v_b) = k_b \nabla^2 T_b \tag{16}$$

where k_b is the thermal conductivity.

No conductance term is included in Eq. 15. Particle diffusion there is the mechanism for enthalpy transport, while interparticle contact and radiant exchange provide conductance for the bulk. The thermal conductivity of Eq. 16 may be estimated by the method of Schotte (1960).

Common simplifications

It is possible to simplify problem descriptions in several ways in order to expedite solution procedures. We will generally assume that bulk density, $n_b = 6(1-\epsilon)/\pi\sigma^3$, is a constant. This overlooks attrition and other factors that reform the particle size distribution during residence in the kiln. It also neglects repacking phenomena in the bulk arising from progress of the reaction and any inflation of the bulk phase owing to release of gaseous reaction products.

We further assume that total density on the top plane depends only on x. This is not valid if rotational rate is time-dependent or if changes of vessel radius or fraction of the cross section filled as functions of the axial coordinate are considered. In addition, we ignore the periodic nature of density arising from the layer-by-layer transport of bulk solid to the top plane. This is a small effect, and it probably is smoothed in any case by the unpredictable triggering of the fall of each layer as its uppermost particles are rotated into unstable positions on the plane. As in the case of the bulk phase, any expansion or fluidization because of interaction with gases must be defined separately.

Similarly, the gas flow is not considered to be sufficiently brisk to transport particles in the top plane, and the y components of particle velocity there and in the bulk are expected to be equal. The top plane is considered to be carried axially by the bulk flow. Because the bulk is in plug flow, we ordinarily treat $v_y = v_{by}$ as constant.

One result of these assumptions is that Eq. 5 may be integrated to give the x component of velocity. Thus, we may abbreviate the equation of continuity to

$$\frac{\partial (nv_x)}{\partial x} = N = \left[\frac{12(1-\epsilon)\Omega}{\sigma^3}\right] x \tag{17}$$

Figure 1 suggests a boundary condition at the point $x=\ell$. At this upper limit of the top plane the rotating vessel contributes to the x component of particle flux by an amount proportional to the cosine of the angle $\beta/2$. The contribution is positive, but particles may be assumed to reflect immediately and elastically from the wall. Hence, $(nv_x)|_{x=\ell} = -2\pi\Omega R n(\ell)\cos(\beta/2)$, leading to the integral of Eq. 17

$$nv_x = -2\pi\Omega R n(\ell)\cos\frac{\beta}{2} - 6(1-\epsilon)\frac{\Omega(\ell^2 - x^2)}{\sigma^3} \tag{18}$$

The flux is negative, directed down the plane, for $-\ell \le x \le \ell$ and $\beta \le \pi$. Its magnitude increases for positive x to a maximum at $x=0$, then decreases again so that fluxes at $x = \pm\ell$ are equal.

One can argue that the random nature of cascading of particles tends to smooth $n(x)$ to a linear form, so that the probability of addition and removal of top-plane particles, whichever is appropriate to the value of x, is the same at each position. We may assume, therefore, that

$$n(x) = n_0 + (n_{av} - n_0)\frac{x+\ell}{\ell} \tag{19}$$

which yields n_{av} as the average value on $-\ell \le x \le \ell$. The density $n_0 = n(-\ell)$ may often be zero but is, in general, an arbitrary value which we may include in order to avoid a singular velocity in Eq. 18 and to account for any tendency for particles to gather at the bottom of the system, at $x=-\ell$. Later we also refer to a tracer experiment in which a unit pulse of an identifiable particle component may be placed initially at $x=-\ell$. In this case the first term of Eq. 19 can be written $2n_0\ell\delta(x+\ell)$.

Another helpful form of Eq. 18 is obtained by use of Eq. 19 with $n_0 = 0$, along with the mean particle speed, v_m. This is

$$nv_x = -4\pi R\Omega n_{av}\left\{\cos\frac{\beta}{2} + 0.1194\frac{v_m}{R\Omega}\left[1 - \left(\frac{x}{\ell}\right)^2\right]\right\}. \tag{20}$$

It may sometimes be appropriate to make the assumption that v_x is much greater than v_y, as the relative times of Table 1 suggest might often be the case. The particle flux in the x direction, J_{ix} of Eq. 10a, is dominated by the final term, the convective part. The diffusivity is isotropic on the top plane, but as the result of the rapid downward, lateral motion compared to that in the axial direction we may for some circumstances wish to consider $\partial n_i/\partial x$ and $\partial^2 n_i/\partial x^2$ to be small relative to the corresponding derivatives with respect to y.

Applications

Isothermal mixing and dispersion processes

There have been many studies of mixing in kilns. Most are either batch studies, in which an initial configuration of tracer particles is followed with respect to time, or continuous, axial dispersion experiments involving addition of tracers with the kiln feed stream. No chemical reactions are considered to occur.

The prior studies utilize one-dimensional balance equations based on the bulk flow. In the following we examine the assumptions needed to obtain such models from multidimensional descriptions.

We assume that for both kinds of mixing experiments the velocities are known. Thus, for the bulk phase, assumed to be in plug flow, if F is the volumetric feed rate, then $v_{by}=F/f\pi R^2$. If, in addition, rotation is assumed to be rigid, $v_{b\theta}=r\Omega$ and $v_{br}=0$.

For the top plane we take $v_y=v_{by}=F/f\pi R^2$, with v_x given by Eq. 18. Because we treat fraction filled, f, as a constant, v_y is also constant and $\partial v_y/\partial y=0$. Equations 6 and 19 apply to $n(x)$, yielding $\partial n/\partial x=2.471\ (1-\epsilon)\Omega\ell^{1/2}/[\sigma^3(g\ \sin\ \alpha)^{1/2}] - n_o/\ell$ with $\partial^2 n/\partial x^2=0$. We also set $\partial n/\partial y=0$.

Proceeding to Eqs. 5 and 13 for the top plane, we assume at first only that $\partial n/\partial t=0$. Then Eq. 5 may be used to derive the identity,

$$n_i(\nabla\cdot v)=\frac{n_i}{n}\left[N-v_x\left(\frac{\partial n}{\partial x}\right)-v_y\left(\frac{\partial n}{\partial y}\right)\right]$$

On substitution in Eq. 13 we find for the case of no chemical reaction

$$\frac{\partial n_i}{\partial t}+\frac{n_i N}{n}+v_x\left[\frac{\partial n_i}{\partial x}-\left(\frac{n_i}{n}\right)\left(\frac{\partial n}{\partial x}\right)\right]+v_y\left[\frac{\partial n_i}{\partial y}-\left(\frac{n_i}{n}\right)\left(\frac{\partial n}{\partial y}\right)\right]=nD_i\left[\frac{\partial^2(n_i/n)}{\partial x^2}+\frac{\partial^2(n_i/n)}{\partial y^2}\right]+N\left[H(x)\frac{n_{bi0}}{n_b}+H(-x)\frac{n_i}{n}\right] \quad (21)$$

The most general form of mixing problem may be approached by solution of the two versions of Eq. 21, the first of these for $x<0$. This result, according to our assumption of rigid bulk-phase rotation, provides bulk-phase composition (number fraction of species i) as a constant equal, say, to $n_i(-x,y,t)/n(-x,y,t)$, on a helical arc extending at constant r_0 from $(-x,y)$ on the negative top plane to $(x,y+v_{by}\tau)$ on the positive side. The top-plane composition for negative x thus

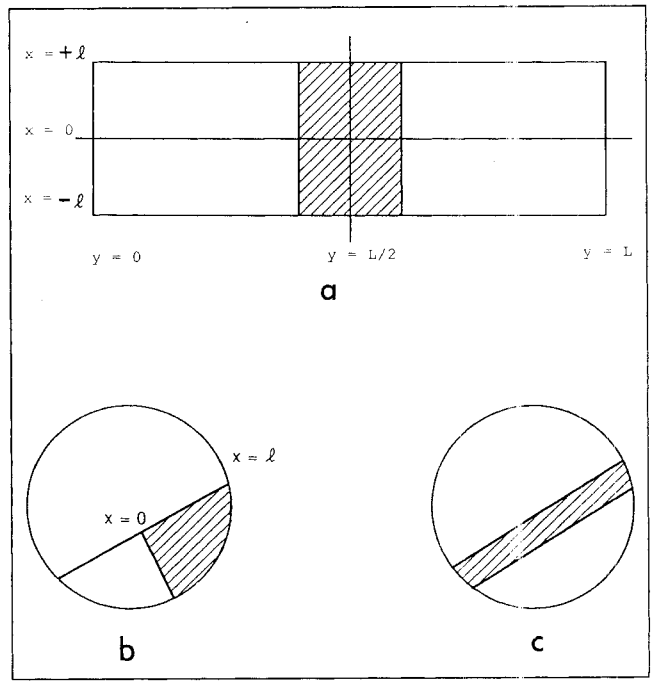

Figure 3. Initial states for isothermal dispersion and mixing studies with binary mixtures including dark tracer particles.

a. Initial state dependence on y, perhaps also on r
b. Initial state dependence on x and θ
c. Initial state dependence on r and θ

turns into n_{bi0}/n_b, and with this number available the solution of Eq. 21 for $x>0$ can proceed.

Various initial conditions lead to specific problem forms. Figure 3a suggests an experiment in which the initial state has tracer particles arranged to depend on y but not on x. Because of the relatively rapid dispersion in the x direction, we might suppose that the initial lack of dependence on x continues for positive times. That is, we consider the number fraction of species i, n_i/n, to be a function only of y and t, for which case we find $\partial n_i/\partial x-(n_i/n)(\partial n/\partial x)=0$. For the same reason, and because $n(x)$ is linear in x, we determine that $\partial^2 n_i/\partial x^2=0$. Typically, for this kind of experiment no feed is used, so that $v_{by}=v_y=0$. We might also suppose that we are interested in conditions at times large enough that the maximum rotational time, $\tau(\ell)=\beta/2\pi\Omega$, is small compared to t. Then

$$\frac{n_{bi0}}{n_b}=\frac{n_i(-x,y-v_{by}\tau,t-\tau)}{n(-x,y-v_{by}\tau,t-\tau)}\approx\frac{n_i(x,y,t)}{n(x,y,t)} \quad (22a)$$

and a single diffusion equation for n_i results from Eq. 20, irrespective of the sign of x:

$$\frac{\partial n_i}{\partial t}=D_i\frac{\partial^2 n_i}{\partial y^2} \quad (22b)$$

In an experiment we would sample the bulk composition, n_{bi}, as a function of y at some value of t. As in the general case described previously, we obtain $n_{bi}(r,\theta,y,t)$ from $n_i(-x,y,t)$, that is, from solution of Eq. 22b. Effectively, either n_i or n_{bi} can be the dependent variable of Eq. 22b. The

solution for boundary conditions such as $\partial n_i/\partial y = 0$ for $y = 0$ and $y = L$ resembles a Gaussian distribution. Together with experimental data, it has provided measurements of D_i (Hogg et al., 1966, 1969; Singh, 1978). The assumptions employed are reasonable, and the resulting diffusivities are correlated by Eq. 11a and otherwise appear faithfully to represent D_i of Eq. 10a.

Figure 3b refers to a study of transverse diffusion and convective mixing. If $v_y = 0$, or if we specify that $n_i/n = \phi(x,t)$, independent of y, and if again $n_{bi0}/n_b \approx n_i/n$, meaning that the fraction of tracer rising to the top plane by rotation is nearly equal to the fraction on the surface, then Eq. 21 resolves to

$$\frac{\partial \phi}{\partial t} + U\frac{\partial \phi}{\partial x} = D_i \frac{\partial^2 \phi}{\partial x^2} \tag{23}$$

where $U(x) = v_x - (2D_i/n)(\partial n/\partial x)$. Equation 23 is to be solved with an initial state similar to that of Figure 3b and boundary conditions such as $\partial\phi/\partial x = 0$ for $x = \pm\ell$. If $D_i = 0$ and there is consequently no diffusion, ϕ, the fraction of tracer, remains constant along trajectories. Photographs of a cross section would show no changes in pattern with respect to time. Top-plane diffusion does occur, however, and the tracer is eventually blended uniformly.

This example is important in that it demonstrates that the transverse diffusion coefficient is identical to that for axial diffusion. Rapid convection down the plane speeds the transverse mixing process, however, as several studies show (Heinen et al., 1983; Hogg and Fuerstenau, 1972; Lehmberg et al., 1977; Wes et al., 1976).

Figure 3c refers to an initial state that is independent of both x and y on the surface but depends on r and θ in the bulk. This case is different from the others in that the beginning of rotation immediately displaces tracer from the positive region and causes n_i/n to depend strongly on x and θ. The initial condition represented by Figure 3c is not a guide to later states, but a new initial condition representing a pulse of tracer located at $x = -\ell$; for example, $2n_0\ell\delta(x+\ell)$, as noted in connection with Eq. 19, may be used. The problem then takes a form similar to that of Eq. 23 and its boundary conditions. A few turns of the kiln have been shown photographically to result in significant smoothing of such an initial configuration (Lehmberg et al., 1977).

Axial dispersion experiments are carried out with continuous axial flow and with tracers added at the inlet end, say as pulses distributed evenly with respect to x. The problem resolves to solution of a suitable version of Eq. 21 for the number fraction of tracer species for $x < 0$,

$$\frac{\partial \psi^-}{\partial t} + v_y\frac{\partial \psi^-}{\partial y} = D_i \frac{\partial^2 \psi^-}{\partial y^2} \tag{24}$$

where $\psi^-(y,t) = n_i/n$. We may assume that the kiln is initially free of tracer and that the inlet pulse has a delta function form. It is convenient to consider the kiln infinite in length, with zero concentration at infinity, evaluating the solution at $y = L$ for comparison with experimental data on exit concentration.

It is of interest in this case to solve the problem fully in order to examine the validity of some of the simplifications that might be employed. Equation 24, with the initial condition $\psi^-(y,0) = 0$ and the boundary conditions, $\psi^-(\infty,t) = 0$, $\psi^-(0,t) = \delta(t)$, has the solution for $x < 0$,

$$\psi^-(y,t) = \frac{y}{2\pi^{1/2}D_i^{1/2}t^{3/2}}\exp\left[-\frac{(y-v_yt)^2}{4D_it}\right] \tag{25}$$

For $x > 0$ one uses the differential equation,

$$\frac{\partial \psi^+}{\partial t} + \frac{N}{n}\psi^+ - \frac{n_{bi0}}{n_b} + v_y\frac{\partial \psi^+}{\partial y} = D_i\frac{\partial^2 \psi^+}{\partial y^2} \tag{26}$$

with the same initial and boundary conditions. From Eq. 22a we deduce that

$$\frac{n_{bi0}}{n_b} = \psi^-(y - v_y\tau, t-\tau) \tag{27}$$

where $\tau = \tau(x)$ is given by Eq. 3 and we use Eq. 25 for the desired functional form. It is clear from this that the assumption that $\psi = n_i/n$ depends only on y and t is an approximation that may be justified by limiting consideration to relatively large process times. In the following we avoid x-dependence of τ, setting $\tau = \beta/2\pi\Omega$, the maximum value on $-\beta/2 \le \theta \le \beta/2$, in order to examine the largest effect of time delay. The solution may be written in terms of $\eta = y - v_yt$ as:

$$\psi^+(\eta,t) = \left(\frac{\eta}{2\pi^{1/2}D_i^{1/2}t^{3/2}}\right)\exp\left[\frac{-(\eta - v_yt)^2}{4D_it}\right]\left\{\exp\left(\frac{-Nt}{n}\right) - \left[\frac{t}{(t-\tau)}\right]^{3/2}\left[\exp\left(-\frac{N(t-\tau)}{n}\right) - 1\right]\exp\left[-\left(\frac{\tau}{4D_i}\right)\left(\frac{\eta^2}{t(t-\tau)} - v_y^2\right)\right]\right\} \tag{28}$$

From this we readily see that the second term of Eq. 26—the term relating composition of the rotated flow onto the top plane to that already on the plane—is zero if the quantity $\{\ldots\}$ of Eq. 28 is unity, so that $\psi^-(\eta, t-\tau) = \psi^+(y,t)$. Such conditions occur in Eq. 28 for $t \gg \tau$ or, equivalently, for $\tau \to 0$. If the kiln is indeed operated less than half full, then τ may be quite a short time compared to the value of t that one might use experimentally. Hence, when $t \gg 1/2\Omega$, we expect that ψ^+ and ψ^- will both be determined by Eq. 24, leading to the solution given by Eq. 25.

The bulk concentration is sampled experimentally. We see that analysis of such samples can again lead to D_i or to other measures of mixing effectiveness (Abouzied et al., 1974; Hogg et al., 1974; Mu and Permutter, 1980; Rutgers, 1965; Wes et al., 1976).

Temperature distributions

In order to illustrate use of the heat balances we consider here a stable, pure, particulate material, so that in Eq. 15 $I = 1$ and $D_i \equiv 0$. Particle mass is m, and the specific heat is c. We also assume constant density in the bulk and that Eq. 17 holds for the top plane. Top-plane and bulk energy equations may then be written in the forms

$$\frac{\partial T}{\partial t}+(v\cdot\nabla)T=\frac{N}{n}[H(x)T_{b0}+H(-x)T-T]+\frac{Q}{mcn} \quad (29)$$

$$\frac{\partial T_b}{\partial t}+(v_b\cdot\nabla)T_b=\alpha_b\nabla^2T_b \quad (30)$$

where $\alpha_b=k_b/n_bmc$. The vector operations are, respectively, two- and three-dimensional for Eqs. 29 and 30. The quantity T_{b0} is the bulk temperature at the point of emergence onto the top plane.

The illustrations we employ refer to batch systems (no axial particulate feed and discharge, so that $v_y=v_{by}=0$). To simplify integrations of Eq. 29 we find it helpful to use the transformations

$$b(x)=\int_0^x\left(\frac{1}{v_x}\right)dx' \quad (31a)$$

and

$$\mu=t-b \quad (31b)$$

for top-plane descriptions. Then for $x\le 0$ Eq. 29 resolves to

$$\frac{\partial T^-}{\partial b}=q(b,\mu+b) \quad (32)$$

and for $x\ge 0$,

$$\frac{\partial T^+}{\partial b}=q(b,\mu+b)+\nu(T_{b0}-T^+) \quad (33)$$

where $q=Q/mcn$ and $\nu=N/n$. One appropriate boundary condition is

$$T^-(0,t)=T^+(0,t)=T_\infty(t) \quad (34a)$$

where we define T_∞ as the center temperature of the plane.

One more condition is needed, most likely referring to an end of the plane. For example, we might assume that the particulate layer of the bulk nearest the wall attains the wall temperature at $x=\ell$. In this case

$$T^+[b(\ell),\mu(\ell)]=T_w(\beta/2,t) \quad (34b)$$

where $T_w(\theta, t)$ is the temperature of the vessel wall and $\mu(\ell)=t-b(\ell)$.

The top-plane equations can then be integrated to

$$T^-(b,\mu)=T_\infty(\mu)+\int_0^b q(b',\mu+b')db' \quad (35a)$$

$$T^+(b,\mu)=T_w\exp\left[\int_b^{b(\ell)}\nu\,db'\right]-\int_b^{b(\ell)}[q(b',\mu+b')+\nu(b')T_{b0}(b',\mu+b')]\exp\left[-\int_{b'}^b\nu\,db''\right]db' \quad (35b)$$

We may simplify these if we recognize that $\exp[\int_0^b \nu\,db']=\exp[\int_0^x(N/nv_x)dx']=\exp\{\int_0^x[\partial\ln(nv_x)/\partial x']dx'\}=nv_x/(nv_x)|_{x=0}$, where we use Eq. 17. We find, with the aid of Eq. 20,

$$T^-(x,t)=T_\infty(t)-\left(\frac{1}{4\pi R\Omega n_{av}}\right)\int_0^x\left\{\left(\frac{Q}{mc}\right)\Big/\left[\cos(\beta/2)-0.1194\left(\frac{v_m}{R\Omega}\right)\left(\left(\frac{x'}{\ell}\right)^2-1\right)\right]\right\}dx' \quad (36a)$$

$$T^+(x,t)=\left[\frac{(nv_x)|_{x=\ell}}{nv_x}\right]T_w\left(\frac{\beta}{2},t\right)-\left(\frac{1}{nv_x}\right)\int_x^\ell\left(\frac{Q}{mc}+NT_{b0}\right)dx' \quad (36b)$$

For the cases in which mc is a constant and the heat delivered to the top plane is independent of position, $Q/mc=$ constant, so that

$$T^-(x,t)=T_\infty(t)-\frac{Q^*\ell}{2\ell^*}\ln\left(\frac{\ell^*+x}{\ell^*-x}\right) \quad (37)$$

where

$$Q^*=\frac{0.6665Q}{mcv_mn_{av}} \quad (38)$$

and

$$\frac{\ell^*}{\ell}=\left(1+8.38\,\frac{\Omega R}{v_m}\cos\frac{\beta}{2}\right)^{1.2} \quad (39)$$

The last number is close to unity for conditions such as those of Table 1. Also

$$T^+(x,t)=\left[\frac{(nv_x)|_{x=\ell}}{nv_x}\right]T_w\left(\frac{\beta}{2},t\right)-(\ell-x)\frac{Q}{mcnv_x}-\left(\frac{1}{nv_x}\right)\int_x^\ell NT_{b0}\,dx' \quad (40)$$

According to Eq. 34a we may equate results at $x=0$ so as to determine the center temperature,

$$T_\infty(t)=\frac{(1/4\pi\Omega Rn_{av})\int_0^\ell(Q/mc+NT_{b0})\,dx'+T_w(\beta/2,t)\cos(\beta/2)}{0.1194v_m/R\Omega+\cos(\beta/2)} \quad (41)$$

This actually represents the temperature of much of the bulk phase, according to experimental results of Barr et al. (1988) and others. We later make use of the value to define the driving force for heat transfer from wall to bulk.

The complete solution requires that T_{b0} be employed in Eqs. 36b and 40, and the heat conduction equation for the bulk,

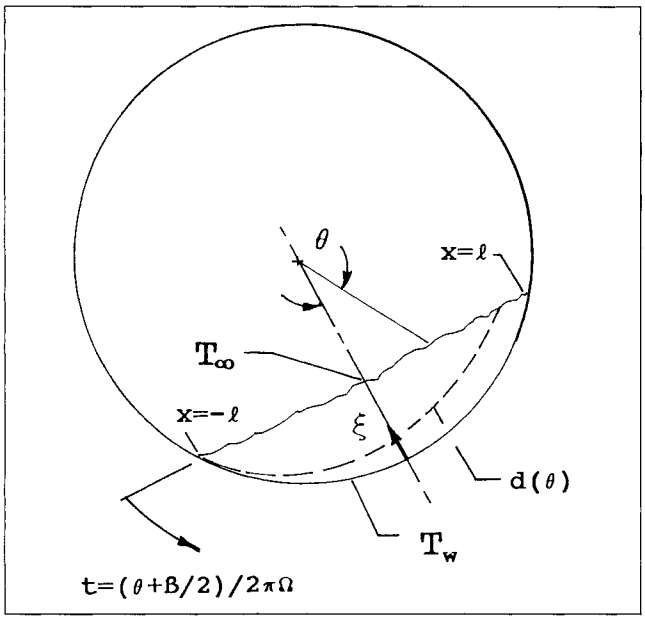

Figure 4. Conditions for a penetration-theory model of wall-to-bed heat transfer.

Penetration depth indicated as a function of θ by - - - and function $d(\theta)$

Eq. 30, must be solved. New auxiliary conditions are required, and we next consider an example.

Modified penetration model for wall-bed heat transfer

Suppose that the kiln is heated externally, and a cooler gas is passed axially through the vessel. In the absence of chemical reaction such a process might represent a kind of moving, pebble-bed heat exchanger in which the particles form an extended surface (Wes et al., 1976). We examine steady-state heat transfer in terms of a model based on concepts from penetration theory.

Referring to Figure 4, we suppose that the vessel radius can be considered to be large compared to the penetration depth, $d(\theta)$, developed as indicated during the period of contact between vessel wall and bed. A time variable, $t=(\theta+\beta/2)/2\pi\Omega$, is zero at the instant of initial wall-bed contact, at $x=-\ell$ and $\theta=-\beta/2$. Time assumes its maximum value, $\beta/2\pi\Omega$, when the rotating vessel wall ceases to contact the solid at $x=\ell$ and $\theta=\beta/2$.

For these conditions, during $0\le t\le\beta/2\pi\Omega$, we define $\xi=R-r$. It is helpful to eliminate the time variable in favor of θ, so that the problem may then be phrased in the form,

$$2\pi\Omega\,\frac{\partial T_b}{\partial\theta}=\alpha_b\,\frac{\partial^2 T_b}{\partial\xi^2} \tag{42}$$

$$T_b(0,\theta)=T_w \tag{43a}$$

$$T_b[R-(R^2-\ell^2)^{1/2},\theta]=T_\infty \tag{43b}$$

$$T_b[\xi,\theta_0(\xi)]=T^-[-(\xi^2-2R\xi+\ell^2)^{1/2},\infty] \tag{43c}$$

where $t\to\infty$ denotes the steady-state form and

$$\theta_0(\xi)=-\cos^{-1}\frac{(R^2-\ell^2)^{1/2}}{(R-\xi)} \tag{43d}$$

for $0\le\xi\le R-(R^2-\ell^2)^{1/2}$.

The initial state, given by Eqs. 43c, d, is altered during the period of rotation by contact with the wall, assumed in this case to have the constant temperature, T_w. (That is, the capacity for external firing is sufficiently large that no cooling of the vessel wall during contact need be considered. In this way we focus on conditions within the vessel.) We wish to solve for the temperature profile and history, then to use these results to characterize the heat transfer coefficient at the wall.

Equation 43a declares that the temperatures of wall and bed are equal when they are in contact. It has been argued that, at least for small particles, the gaseous mean free path next to the wall is sufficiently long that convective and conductive exchange cannot equilibrate the two surfaces locally (Schlünder, 1971). Radiation plays a role, of course. Nevertheless, Lehmberg et al. (1977) concluded from their use of a penetration model that equal wall and bed temperatures led to excessively large estimates of wall-to-bed heat transfer coefficients. They postulated a small gap between wall and bed over which a temperature jump occurs. The gap turned out to be much greater than the mean free path of the gas, and Schlünder's model was not considered to be appropriate. Rather the authors supposed that a gas layer of thickness slightly greater than the diameter of a particle presents the next-to-wall resistance to heat transfer.

Tscheng and Watkinson (1979) also considered their estimates of heat transfer coefficient based on equal wall and bed temperatures to be high compared to the various data they were able to examine, accepting the explanation that a gas film at the wall impedes heat transfer. On the other hand the model of Schlünder (1971) was adopted by Barr et al. (1989) in their recent study of various paths of heat exchange in a pilot-scale kiln.

In the present work we begin by using Eq. 43a in order to investigate the effects of top-plane particle flow on the predictions of the penetration theory. The result should represent an improved application of the theory and give a better basis for examination of the argument that a temperature jump of significant magnitude may occur at the wall.

An overall heat balance may be written in the form

$$h_{wb}\beta R(T_w-T_\infty)=-2\ell Q \tag{44}$$

where we have chosen the area with which to define the heat transfer coefficient, h_{wb}, to be that of the wall in the region of wall-to-bed contact. Utilizing this definition and the result of Eq. 37, we may rewrite the initial condition, Eq. 43c, as

$$\Phi[\xi,\theta(\xi)]=1+S\ln\left[\frac{\ell^*-(\xi^2-2R\xi+\ell^2)^{1/2}}{\ell^*+(\xi^2-2R\xi+\ell^2)^{1/2}}\right] \tag{45}$$

where we define $\Phi(\xi,\theta)=[T_b(\xi,\theta)-T_w]/(T_\infty-T_w)$ and where $S=[h_{wb}/mcN(\ell)][(\beta/2)/\sin(\beta/2)]$ is a Stanton number, a ratio of heat fluxes, that of wall-to-bed heat transfer divided by that of particulate convection from bulk to top plane. It is then helpful to rephrase the problem in terms of $\Phi(\xi,\theta)$:

$$\partial\Phi/\partial\theta = \left(\frac{\alpha_b}{2\pi\Omega}\right)\left(\frac{\partial^2\Phi}{\partial\xi^2}\right) \tag{46}$$

$$\Phi(0,\theta) = 0 \tag{47a}$$

$$\Phi[R-(R^2-\ell^2)^{1/2},\theta] = 1 \tag{47b}$$

with the initial condition given by Eq. 45.

Equations 45-47 may be solved by setting $\Phi(\xi,\theta) = \Phi_0(\xi,\theta) + S\Phi_1(\xi,\theta)$. The first of the unknown functions is given by

$$\frac{\partial\Phi_0}{\partial\theta} = \left(\frac{\alpha_b}{2\pi\Omega}\right)\left(\frac{\partial^2\Phi_0}{\partial\xi^2}\right) \tag{48}$$

$$\Phi_0(0,\theta) = 0 \tag{49a}$$

$$\Phi_0(\infty,\theta) = 1 \tag{49b}$$

$$\Phi_0\left(\xi, \frac{-\beta}{2}\right) = 1 \tag{49c}$$

In Eq. 49b we have used the condition $R \gg d(\theta)$ to make the simplification that $R-(R^2-\ell^2)^{1/2}$ might be taken to be large when $S \to 0$, appropriate for study of $\Phi_0(\xi,\theta)$. The condition of Eq. 49c is a version of Eqs. 43c,d which fixes the temperature of the entire negative top plane at T_∞ as a condition on determination of Φ_0.

Equations 48–49 yield

$$\Phi_0(\xi,\theta) = \operatorname{erf}\frac{\pi^{1/2}\xi}{2d(\theta)} \tag{50}$$

with $d(\theta) = [(\theta+\beta/2)\alpha_b/2\Omega]^{1/2}$. This is identical to the result one would obtain from the conventional assumptions of penetration theory, which replace radial transport by linear flow and provide boundary conditions appropriate to a similarity solution such as that of Eq. 50.

For $\Phi_1(\xi,\theta)$ the same differential equation applies,

$$\frac{\partial\Phi_1}{\partial\theta} = \left(\frac{\alpha_b}{2\pi\Omega}\right)\left(\frac{\partial^2\Phi_1}{\partial\xi^2}\right) \tag{51}$$

with the boundary and initial conditions,

$$\Phi_1(0,\theta) = 0 \tag{52a}$$

$$\Phi_1[R-(R^2-\ell^2)^{1/2},\theta] = 0 \tag{52b}$$

$$\Phi_1[\xi,\theta(\xi)] = \ln\left[\frac{\ell^* - (\xi^2 - 2R\xi + \ell^2)^{1/2}}{\ell^* + (\xi^2 - 2R\xi + \ell^2)^{1/2}}\right] \tag{52c}$$

We obtain periodic boundary conditions, Eqs. 52a,b, in this case by choosing the maximum of ξ, instead of the infinite value, for use in Eq. 52b. The solution for the case $R \gg d(\theta)$ is

$$\Phi_1(\xi,\theta) = \sum_{j=1}^{\infty} \omega_j \sin(\lambda_j\xi)\exp\left[-\frac{\lambda_j^2\alpha_b\theta}{2\pi\Omega}\right] \tag{53}$$

where $\lambda_j = j\pi/[R-(R^2-\ell^2)^{1/2}]$. The coefficients, ω_j, are to be obtained from Eq. 52c, and for $R \gg d(\theta)$ this is feasible in terms of a conventional Fourier sine expansion.

The combined solution is

$$\Phi(\zeta,\theta) = \operatorname{erf}\frac{\pi^{1/2}\zeta}{2\Delta} + 2S\sum_{j=1}^{\infty} B_j(\beta)\exp(-j^2\pi\zeta^2)\sin(j\pi\zeta) \tag{54}$$

where

$$\zeta = \frac{\xi}{R-(R^2-\ell^2)^{1/2}} \tag{55a}$$

$$\Delta(\theta) = \frac{d(\theta)}{R-(R^2-\ell^2)^{1/2}} \tag{55b}$$

and

$$B_j(\beta) = \int_0^1 \sin(j\pi\zeta)\ln\left[\frac{\ell^*/\ell + \chi(\zeta)}{\ell^*/\ell - \chi(\zeta)}\right]d\zeta \tag{56a}$$

with

$$\chi(\zeta) = \frac{a_2(\zeta^2 - 2\zeta/a_2 + a_1/a_2)}{\sin(\beta/2)} \tag{56b}$$

and $a_1 = 1+\cos(\beta/2)$, $a_2 = 1-\cos(\beta/2)$.

The heat balance of Eq. 44 may now be reformulated as

$$Rk_b(T_w - T_\infty)\int_{-\beta/2}^{\beta/2}\left(\frac{\partial\Phi}{\partial\xi}\right)\Bigg|_{\xi=0} d\theta = h_{wb}R\beta(T_w - T_\infty)$$

On rearranging and utilizing Eq. 54 we find for the Nusselt number, $Nu = h_{wb}R\beta/k_b$,

$$Nu = \frac{2\sqrt{2}\,P^{1/2}}{1+\sum_{j=1}^{\infty}\left[\frac{B_j(\beta)}{\pi a_1}\right]\left[1-\exp\left(\frac{-j^2\pi\beta}{2Pa_2^2}\right)\right]} \tag{57}$$

in terms of the Peclet number, $P = R^2\beta\Omega/\alpha_b$.

The Nusselt number for wall-to-bed heat transfer is determined by Eq. 57 as a function of the fraction of the vessel filled, expressed by the angle, β, of the Peclet number and of the reduced mean particle velocity on the top plane, $v_m/R\Omega$, which is used to determine ℓ^*/ℓ as in Eq. 39.

If the Peclet number is large, the sum in the denominator of Eq. 57 does not contribute, and we find the prediction, $Nu = 2\sqrt{2}P^{1/2}$, when the boundary condition of Eq. 43a is used, that is, if the bed and wall have the same temperature when they are in contact. This is the result obtained by means of conventional penetration theory illustrated in prior studies, for example, by Lehmberg et al., (1977) and by Tscheng and Watkinson (1979).

Figure 5 is a comparison of values calculated from the present work, utilizing Eq. 57, with other penetration theory forms. The points shown are based on a figure of Tscheng and Watkinson (1979), where the original sources are identified. The

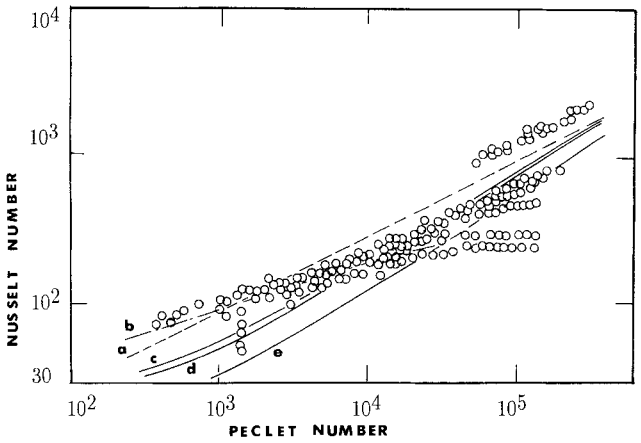

Figure 5. Wall-to-bed heat transfer.

o Experimental data of Tscheng and Watkinson (1979)
a. Conventional penetration theory, $Nu = 2^{3/2}P^{1/2}$
b. Empirical form of Tscheng and Watkinson, $Nu = 11.6\ P^{0.3}$
c. Present calculations, $\Omega R/v_m = 0.05$, $\beta \leq 110$ degrees
d. $\beta = 140$ degrees
e. $\beta = 180$ degrees

current predictions are lower than those from conventional penetration theory, and they are as a result in better agreement with the experimental results. The explanation comes from recognizing that rotation of particles from bulk to top plane assists heat transfer. Hence, for a given heat load one requires and predicts a smaller heat transfer coefficient than is the case if the rotational flux is not considered.

There does not appear to be justification, therefore, for postulating an air gap at the vessel wall as the explanation for experimental Nusselt numbers smaller than those predicted by conventional penetration theory. Instead we find in the present problem form that the steady state is maintained by the loss of heat from the top plane to the gas phase, in an amount identical to that transferred to the particle bed from the wall. It is the heat flow from the top plane that lowers the net heat flux, hence decreases the calculated heat transfer coefficient.

For Peclet numbers below 10^4 Tscheng and Watkinson (1979) recommend the empirical form, $Nu = 11.6P^{0.3}$, basing this on all of the published data available at the time.

The apparent scatter for large Peclet numbers in Figure 5 is not entirely the result of experimental errors. We have seen that Nusselt numbers cannot be represented solely as a function of the Peclet number. We must specify degree of fill, representing angle β, as well as the reduced time, $\Omega R/v_m$. Thus, for Peclet numbers of about 10^5 there is segregation of the experimental results into horizontal groups. There is qualitative agreement between experiment and prediction, in the sense that the lower horizontal groups of points correspond to larger particle sizes, probably consistent with large fraction of vessel filled. Further detailed comparisons are hampered by the need for additional experimental information.

Discussion

The particulate flow through a rotary kiln has been treated here as occurring in two distinct regions, an axial, bulk portion moving quite slowly and a faster, lateral flow across the top of the axial stream, produced by rotation of the vessel. If the kiln is operated considerably less than half full of particles, then an element of solid may move frequently between the flows, crossing the top plane several times during each revolution of the vessel.

Axial particle diffusion is superimposed on the lateral, top-plane flow. Despite the short residence time on this plane experienced by a particle moving directly laterally at the mean particle speed, impediments to free flow, such as collisions, distribute residence times broadly and lengthen particle trajectories on the top plane.

Coupling of the bulk and top-plane regions assists any process involving significant radial fluxes. This, as we have shown, is the case for heat transfer from an external source to the axial gas flow, by way of the particulate mass. Such assistance would also be observed for calcination and for pyrolysis, whenever gas–solid interaction is important in determining the rate of a process. Turnover of particles through the top plane brings particulate and gas phases into close contact. Diffusion on the top plane assists by prolonging residence time there. Excessive top-plane diffusion can decrease rates, of course, if overall performance depends strongly on plug flow of the solid.

Mixing processes also depend critically on top-plane behavior, for dispersion of particle species is severely limited if top-plane diffusion is in some way curtailed. It is important to realize, however, that vessel internals that do not protrude through or into the top plane so as to inhibit axial dispersion, are generally beneficial in fostering the cooperative actions of top-plane and bulk regions.

When mixing involves particle types that can interact in some fashion—for example, by heat or mass exchange, perhaps by solid–solid reaction—then the bulk phase has special importance, because it provides the most intimate particle–particle contact, disturbed rather little by other vessel processes. Even in these circumstances, however, the rearrangements of particles that accompany frequent movement into and out of the top plane contribute positively to overall rates. Without such reformation of particulate structures in the bulk, driving forces between adjacent particle surfaces eventually would become too small to support suitably rapid changes.

Problem-solving is aided by breaking the top plane into two parts. That for $x > 0$, above the midpoint, is coupled to the bulk properties by the flow of solid from bulk to top plane. For $x < 0$, however, in the region below the midpoint, the species and enthalpy equations involve only top-plane variables.

Thus, a problem is generally best attacked by first considering the top-plane equations for negative x. The result is composition or temperature, for example, of the particles that must be captured by the bulk and rotated around to positive x. One thus obtains initial or boundary conditions for solution of the bulk equations, which in turn yield values to be incorporated into the top-plane equations for positive x. Identification of the top-plane forms at the midpoint, $x = 0$, completes the procedure.

Problems may be simplified in a number of ways, loosening the otherwise strongly coupled bulk and top-plane descriptions. When they are used fully, the various assumptions produce problem descriptions identical to those that would be constructed if the solid flow were considered to be in a single, axially directed stream. This is reassuring. But it also illustrates that one needs discretion in applying simplifications so that the important top-plane phenomena are not ignored and so

that the interactions of bulk and top plane, essential to the understanding of some processes, are included.

Notation

a = defined by Eq. 56b.
b = time variable, Eq. 31a, s
B = see Eq. 56a
c = specific heat, j/kg·K
d = penetration layer thickness, m
D = particle diffusivity on top plane, m^2/s
f = fraction of vessel volume filled with solid
F = volumetric feed rate of solid, m^3/s
g = acceleration of gravity, m/s^2
h = enthalpy, j
h_{wb} = heat transfer coefficient between wall and bed, $W/m^2 \cdot K$
$H(x)$ = Heaviside step function; zero for $x<0$, unity for $x>0$
J, J_b = particle flux, $m^{-1} \cdot s^{-1}$ or $m^{-2} \cdot s^{-1}$
k = thermal conductivity, w/m·K
ℓ = half-width of top plane, m
ℓ^* = see Eq. 39, m
L = length of kiln, m
m = particle mass, kg
n = surface particle density, m^{-2}
n_b = bulk density, m^{-3}
N = local exchange rate, top plane and bulk, particles/$m^2 \cdot s$
N_p = total exchange rate, particles/s
Nu = Nusselt number for wall-to-bed heat transfer, $h_{wb}R\beta/k_b$
P = Peclet number, $R^2\Omega\beta/\alpha_b$
q = Q/mcn, Eq. 32
Q = heat flux, W/m^2
Q^* = see Eq. 38, W/m^2
r = radial coordinate, m
R = vessel radius, m
R_i, R_{bi} = reaction rates, particles/$m^2 \cdot s$ or particles/$m^3 \cdot s$
S = Stanton number, Eq. 45
t = time, s
T = temperature, K
v = velocity of particle flow, m/s
V^* = rotational turnover number, $(\ell/R)^2/f$
x = lateral coordinate, m
y = axial coordinate, m

Greek letters

α = angle of repose; thermal diffusivity, m^2/s
β = angle subtended by top plane
γ = angle of tilt of kiln
$\delta(x)$ = Dirac delta function
Δ = penetration depth, Eq. 55b
ϵ = void fraction of bulk phase
ζ = depth, Eq. 55a
θ = tangential coordinate
λ = eigenvalue, Eq. 53, m^{-1}
μ = relative time, Eq. 31b, s
ν = N/n, s^{-1}
ξ = $R-r$, m
σ = particle diameter, m
τ = average residence time, s
$\tau(x)$ = rotation time, eq. 3, s
ϕ, ψ = number fraction of a particle type
Φ = dimensionless temperature
χ = defined by Eq. 56b
ω = Fourier coefficient
Ω = rotational rate, s^{-1}

Subscripts and superscripts

av = average value
b = bulk-phase value
i = particle species, $i=1, 2, \ldots, I$
m = mean value
r, θ = polar coordinate axes in bulk
s = sparsely populated limit
rot = average during rotation
top = average for top-plane condition
x, y = lateral, axial coordinate direction
w = value at vessel wall
0 = value of r or θ at top plane
$+, -$ = (superscripts) values for $x>0$, $x<0$
∞ = center temperature

Literature Cited

Abouzied, A.-Z. M. A., T. S. Mika, K. V. Sastry, and D. W. Fuerstenau, "The Influence of Operating Variables on the Residence Time Distribution for Material Transport in a Continuous Rotary Drum," *Powder Technol.*, **10**, 273 (1974).

Bridgwater, J., "Fundamental Powder Mixing Mechanisms," *Powder Technol.*, **15**, 215 (1976).

Barr, P. V., J. K. Brimacombe, and A. P. Watkinson, "A Heat-Transfer Model for the Rotary Kiln. I: Pilot Kiln Trials," *Metall. Trans. B*, **20**, 391; "II: Development of the Cross-Section Model," *ibid.*, 403 (1989).

Heinen, H., J. K. Brimacombe, and A. P. Watkinson, "Experimental Study of Transverse Bed Motion in Rotary Kilns," *Metall. Trans. B*, **14**, 191 (1983).

Hogg, R., D. S. Cahn, T. W. Healy, and D. W. Fuerstenau, "Diffusional Mixing in an Ideal System," *Chem. Eng. Sci.*, **21**, 1025 (1966).

Hogg, R., G. Mempel, and D. W. Fuerstenau, "The Mixing of Trace Quantities into Particulate Solids," *Powder Technol.*, **2**, 223 (1969).

Hogg, R., and D. W. Fuerstenau, "Transverse Mixing in Rotating Cylinders," *Powder Technol.*, **6**, 139 (1972).

Hogg, R., K. Shoji, and L. G. Austin, "Axial Transport of Dry Powders in Horizontal Rotating Cylinders," *Powder Tech.*, **9**, 99 (1974).

Lehmberg, J., M. Hehl, and K. Schuegerl, "Transverse Mixing and Heat Transfer in Horizontal Rotary Drum Reactors," *Powder Technol.*, **18**, 149 (1977).

Mu, J., and D. D. Perlmutter, "The Mixing of Granular Solids in a Rotary Cylinder," *AIChE J.*, **26**, 928 (1980).

Mu, J., and D. D. Perlmutter, "A Simulation Study of Rotary Reactor Performance," *Chem. Eng. Commun.*, **9**, 101 (1981).

Oyama, Y., "Particle Motion in a Horizontal Rotating Cylinder," *Int. Chem. Eng.*, **20**, 36 (1980).

Rutgers, R., "Longitudinal Mixing of Granular Material Flowing Through a Rotating Cylinder," *Chem. Eng. Sci.*, **20**, 1089 (1965).

Schotte, W., "Thermal Conductivity of Packed Beds," *AIChE J.*, **6**, 63 (1960).

Schlünder, E. U., "Wärmeübergang an bewegte Kugelschüttungen bei kurzfristigem Kontakt," *Chemie-Ing.-Techn.*, **43**, 651 (1971).

Singh, D. K., "A Fundamental Study of the Mixing of Solid Particles," PhD Diss., Univ. Rochester, NY, (1978).

Tscheng, S. H., and A. P. Watkinson, "Convective-Heat Transfer in a Rotary Kiln," *Can. J. Chem. Eng.*, **57**, 433 (1979).

Wes, G. W. J., A. A. H. Drinkenburg, and S. Stemerding, "Solids Mixing and Residence Time Distribution in a Horizontal Rotary Drum Reactor," *Powder Technol.*, **13**, 177; 185 (1976).

Manuscript received Dec. 4, 1990, and revision received Mar. 25, 1991.